Journal of
Materials Chemistry

Cite this: *J. Mater. Chem.*, 2011, **21**, 7210

www.rsc.org/materials

PAPER

Pyrene-substituted ethenes: aggregation-enhanced excimer emission and highly efficient electroluminescence†

Zujin Zhao,[ab] Shuming Chen,[c] Jacky W. Y. Lam,[a] Zhiming Wang,[d] Ping Lu,[d] Faisal Mahtab,[a] Herman H. Y. Sung,[a] Ian D. Williams,[a] Yuguang Ma,[d] Hoi Sing Kwok[c] and Ben Zhong Tang*[ae]

Received 20th December 2010, Accepted 15th March 2011
DOI: 10.1039/c0jm04449k

Pyrene-substituted ethenes, 1,2,2-tripheny-1-pyrenylethene (TPPyE) and 1,2-diphenyl-1,2-dipyrenylethene (DPDPyE), are synthesized and characterized. Whereas they are weakly emissive in solution they become strong emitters when aggregated in the condensed phase. In contrast to the general observation that excimer formation quenches the light emission of fluorophores, TPPyE and DPDPyE exhibit efficient excimer emissions in the solid state with high fluorescence quantum yields up to 100%. The π–π intermolecular interactions between the pyrene rings, coupled with multiple C–H⋯π hydrogen bonds, efficiently restrict intramolecular rotations, which block the nonradiative energy decay channel, and hence make the dye molecules highly emissive in the solid state. Non-doped organic light-emitting diodes using TPPyE and DPDPyE as emitters are fabricated, which give green light at low turn-on voltages (down to 3.2 V) with maximum luminance and power, current, and external quantum efficiencies of 49830 cd m^{-2}, 9.2 lm W^{-1}, 10.2 cd A^{-1} and 3.3%, respectively.

Introduction

Advancement in optoelectronics is directly associated with the development of new luminescent materials. Whereas many dyes emit strongly when molecularly dissolved in good solvents, they become weak fluorophores when aggregated in poor solvents or fabricated as thin films in the solid state. In the condensed phase, the dye molecules are located in the immediate vicinity of each other and experience strong intermolecular interactions, which promote the formation of species such as excimers and exciplexes which are detrimental to luminescence. On the other hand, aggregation enables efficient intermolecular charge transfer[1] and can positively restrict the intramolecular rotation (IMR) of the fluorophores,[2] which blocks the nonradiative decay channels, and hence enhances their fluorescence efficiencies. Whether aggregation quenches or strengthens the light emission is determined by the competition between these two antagonistic factors. Unfortunately, the negative effect is dominant in the photoluminescence (PL) process of most luminophors. This is known as aggregation-caused quenching (ACQ) of light emission.[3]

We have recently discovered a phenomenon exactly opposite to the ACQ effect, that is, aggregation-induced emission (AIE): a series of propeller-shaped non-emissive molecules can be induced to emit efficiently by aggregate formation.[4] In solution, they are non-emissive because of the active IMR process, which serves as a relaxation channel for the excited state to decay. In the aggregate state, they are induced to emit intensely owing to the restriction of the IMR process[5,6] and the suppression of the intermolecular interactions by their nonplanar conformations. Among the AIE molecules, tetraphenylethene (TPE) enjoys the advantages of facile synthesis and efficient solid-state emission as well as high thermal stability. A wide variety of substituents has been attached to its phenyl blades to endow it with enhanced and/or new electronic and optical properties. Pyrene is a flat aromatic molecule and shows interesting fluorescence properties.[7,8] It is bulky and rigid and luminophors containing such a chromophore are anticipated to show high fluorescence quantum yield (Φ_F) and thermal stability. In this study, we utilized pyrene as a building block for the construction of new luminogens. We replaced one or two phenyl ring(s) of TPE by pyrene ring(s) and investigated the photophysical properties of the resultant luminogens. We investigated whether pyrene-substituted ethenes, similar to TPE, are AIE-active and if their aggregates are emissive, and attempted to clarify the origins for light emission and causes of the AIE process.

---

[a] *Department of Chemistry, Institute of Molecular Functional Materials, The Hong Kong University of Science & Technology (HKUST), Clear Water Bay, Kowloon, Hong Kong, China. E-mail: tangbenz@ust.hk*
[b] *College of Material, Chemistry and Chemical Engineering, Hangzhou Normal University, Hangzhou, 310036, China*
[c] *Center for Display Research, HKUST, Kowloon, Hong Kong, China*
[d] *State Key Laboratory of Supramolecular Structure and Materials, Jilin University, Changchun, 130012, China*
[e] *Department of Polymer Science and Engineering, Zhejiang University, Hangzhou, 310027, China*

† CCDC reference numbers 755289 (TPPyE) and 755290 (*cis*-DPDPyE). For crystallographic data in CIF or other electronic format see DOI: 10.1039/c0jm04449k

Results and discussion

Scheme 1 illustrates the synthetic routes to the pyrene-substituted ethenes. Detailed procedures and characterization data are given in the Experimental section. Single crystals of TPPyE were grown from a hexane–dichloromethane solution and analyzed by X-ray diffraction crystallography. Crystals of both *cis*- and *trans*-isomers of DPDPyE were obtained by a very slow evaporation of a chloroform solution. Fortunately we were able of isolate crystals of *cis*-DPDPyE from the mixture. The crystal structures and B3LYP/6-31G* calculated molecular orbital amplitude plots of HOMO and LUMO levels of TPPyE and *cis*-DPDPyE are shown in Fig. 1. The electron clouds in both HOMO and LUMO levels of TPPyE and *cis*-DPDPyE are mainly located on the pyrene ring(s), revealing that this chromophoric unit predominantly controls the absorption and emission of the molecules. The thermal properties of TPPyE and DPDPyE were examined by differential scanning calorimetry (DSC) and thermogravimetric analysis (TGA) measurements. The DSC thermograms of TPPyE and DPDPyE revealed melting temperatures at 203 and 279 °C, respectively. No glass-transition temperature, however, was detected. As shown in Fig. 2A, both molecules show high thermal stability and decompose at high temperatures (269 °C for TPPyE and 370 °C for DPDPyE). These values are much higher than that for TPE (224 °C)[5c] owing to the high rigidity and bulkiness of the pyrene ring.

The UV-vis spectrum of TPPyE resembles that of DPDPyE and shows an absorption maximum at ~350 nm (Fig. 2B). The molar absorptivity of DPDPyE at 353 nm (1.9×10^4 M^{-1} cm^{-1}) is about two times higher than that of TPPyE, but is much lower than the value exhibited by pyrene at 335 nm (5.4×10^4 M^{-1} cm^{-1}).[9] The PL spectrum of TPPyE in dilute THF solution (10^{-8} M) displays a sharp peak at 388 nm which well extends to 570 nm (Fig. 3A). When the solution concentration is increased to 10^{-7} M, a new peak is observed at 483 nm. Whereas the former peak (388 nm) is assigned to the monomer emission of the pyrene moiety[7,8] the latter one (483 nm) may be associated with the emission of pyrene excimers. To prove this, we prepared more concentrated solutions, as excimer emission is known to be concentration dependent. With a progressive increase in the solution concentration, the emission at 483 nm becomes dominant, and at 10^{-3} M, only emission at the longer wavelength is observed, demonstrating that it is truly originated from pyrene excimers.[8,10] The same phenomenon is also observed in the spectrum of DPDPyE but at the same concentration the excimer emission in DPDPyE is much stronger. The tendency for excimer formation in DPDPyE is so high that even at a concentration as low as 10^{-8} M, its PL spectrum still exhibits excimer emission at 523 nm (Fig. 3B). The excimer emission of DPDPyE is red-shifted relative to that of TPPyE because two pyrene rings are present in one molecule of DPDPyE, which encourages the formation of J-aggregates through intermolecular π–π stacking. For a 10 μM THF solution, the Φ_F value of TPPyE is 2.8%, of which about 65% is contributed from the excimer. For the same solvent and concentration, DPDPyE has a higher Φ_F value (9.8%), but is still much lower than that of the pyrene monomer (32% in ~50 μM cyclohexane)[9] and most pyrene-substituted luminophors.[11] Such phenomena have been observed in conventional planar luminophors with rotatable phenyl rings and are caused by the active IMR process, which promotes the nonradiative decay of the excited states.[12]

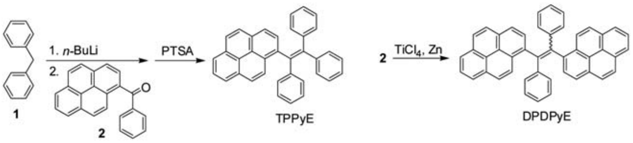

Scheme 1 Synthetic routes to TPPyE and DPDPyE. PTSA = *p*-toluenesulfonic acid.

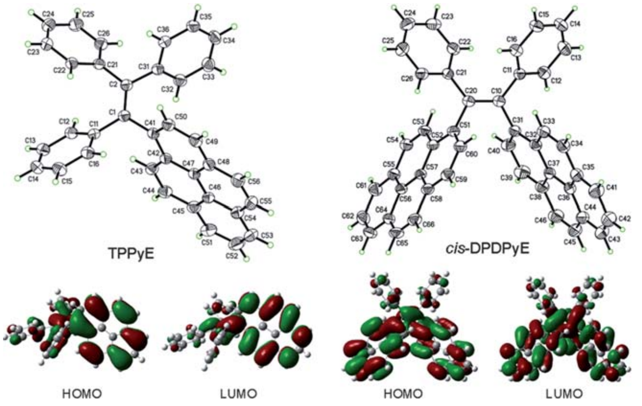

Fig. 1 ORTEP drawings and B3LYP/6-31G* calculated molecular orbital amplitude plots of HOMO and LUMO levels of TPPyE and *cis*-DPDPyE.

We further studied their optical properties in the crystal and amorphous states. Upon photoexcitation, crystals of TPPyE and *cis*-DPDPyE emit at 481 and 486 nm, respectively (Table 1). The PL of the amorphous film of TPPyE is found at 484 nm, which is close to those in concentrated solution and the crystal state (Fig. 4A), suggesting that they originate from the same emitting species with similar molecular interactions. On the other hand, the PL of an amorphous film of DPDPyE is located at 503 nm, which is 17 nm red-shifted from the spectrum of the crystals. The unusual blue shift observed in the crystalline phase may be attributable to conformation twisting in the crystal packing process, during which the DPDPyE molecules may conformationally adjust themselves by twisting their aromatic rings to fit into the crystalline lattice. Without such restraint, the molecules

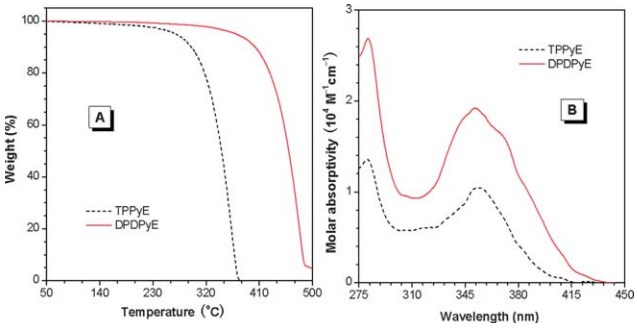

Fig. 2 (A) TGA thermograms for TPPyE and DPDPyE recorded under nitrogen at a heating rate of 10 °C min^{-1}. (B) Absorption spectra of TPPyE and DPDPyE in THF solutions (10 μM).

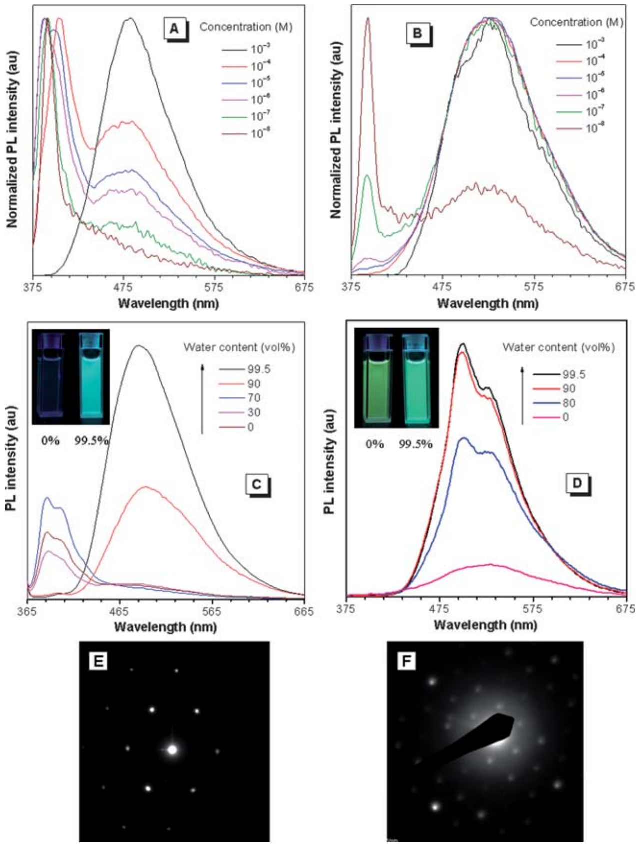

Fig. 3 Normalized PL spectra of (A) TPPyE and (B) DPDPyE in THF solutions with different concentrations. PL spectra of (C) TPPyE and (D) DPDPyE in THF–water mixtures (1 μM) with different water contents. Insets in panels (C) and (D): photographs of TPPyE and DPDPyE in THF and in THF–water (99.5% water content) taken under UV illumination. Excitation wavelength: 350 nm. ED patterns of crystalline aggregates of (E) TPPyE and (F) DPDPyE formed in THF–water with 90% water content.

Table 1 Optical properties of TPPyE and DPDPyE in solution (Soln)[a] and crystalline (Cryst) and amorphous[b] (Film) states

	λ_{abs}/nm	λ_{em}/nm			Φ_F (%)	
	Soln	Soln	Cryst	Film	Soln[c]	Film[d]
TPPyE	353	(388) 483	481	484	2.8	61
DPDPyE	352	(391) 523	486[e]	503	9.8	100

[a] In THF solution (10 μM). [b] Film spin-coated on quartz plate. [c] Quantum yields (Φ_F) determined in THF solutions using 9,10-diphenylanthracene (Φ_F = 90% in cyclohexane) as standard. [d] Quantum yield of the amorphous film measured by an integrating sphere. [e] Crystals of *cis*-DPDPyE.

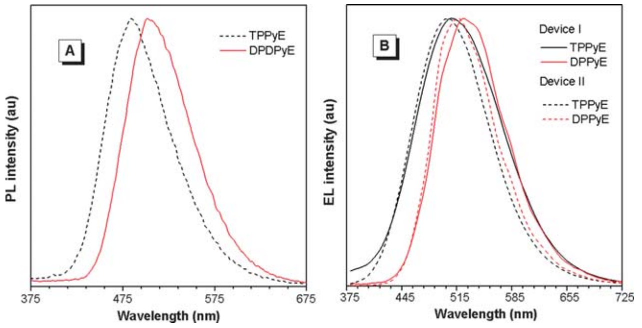

Fig. 4 (A) PL spectra of thin films of TPPyE and DPDPyE and (B) EL spectra of TPPyE and DPDPyE in multilayer devices with configurations of ITO|NPB (60 nm)|emitter (20 nm)|TPBi (30 nm)|LiF (1 nm)|Al (100 nm) (device I) and ITO|NPB (60 nm)|emitter (20 nm)|TPBi (10 nm)|Alq_3 (30 nm)|LiF (1 nm)|Al (100 nm) (device II).

in the amorphous state may assume a more planar conformation, which enables better π–π stacking interactions, and hence results in a red-shifted emission. In concentrated solution, extensive excimers may be readily formed because the molecules can adjust their conformations and locations with little constraint, in order to maximize the intermolecular interactions or overlapping of pyrene rings. This may account for the further red-shift in the emission maximum. In contrast to their weak emission in dilute solutions, the amorphous films of TPPyE and DPDPyE emit more efficiently. Their Φ_F values reach 61 and 100%, respectively, and are much higher than those of pyrene film (44%) and TPE (49.2%)[5c] measured under the same conditions. This demonstrates a novel phenomenon of aggregation-enhanced excimer emission (AEEE) and suggests that replacement of the phenyl ring(s) of TPE by pyrene ring(s) has generated new luminogens with more efficient solid-state emissions.

To further confirm the AEEE feature of TPPyE and DPDPyE, the PL behaviors of their aggregates in poor solvents were investigated. When a large amount of water is added into the THF solutions, their emissions are strengthened. At 90% water content, intense excimer emission was observed in the spectrum of TPPyE at 485 nm. The emission in a 99.5% aqueous mixture is so strong that the monomer emission at ~388 nm is hardly discerned (Fig. 3C). The excimer emission of DPDPyE also becomes stronger in THF–water mixtures with higher water contents (Fig. 3D). Since TPPyE and DPDPyE are not soluble in water, their molecules must be aggregated in solvent mixtures with large amounts of water. The solutions are, however, homogeneous with no precipitates, suggesting that the aggregates are nanodimensional. The discernible vibronic structure in the excimer emission band of DPDPyE (Fig. 3D) is indicative of the formation of extremely structured aggregates as ascertained from the vibronic progression of the C=C stretching mode.[13] The electron diffraction (ED) patterns of the aggregates of TPPyE and DPDPyE formed in 90% aqueous mixtures display many diffraction spots (Fig. 3E and 3F), demonstrating that they are crystalline in nature.

Several papers have reported that the pyrene excimers in the crystal state can emit more efficiently than their monomeric species in solution.[14] Concentration quenching, however, is still a general phenomenon observed in pyrene and its derivatives.[7,8] Although scientists have tried hard to hamper intermolecular interactions, the emission efficiencies of most pyrene-containing luminophors are reduced in solid films and the crystal state.[11] We thus investigated the crystal structures to try and rationalize why an opposite effect is observed in TPPyE and DPDPyE. As shown in Fig. 5, the pyrene rings of two adjacent TPPyE molecules are stacked in a parallel fashion and about half of their surfaces (~7 carbon atoms) are overlapped (Fig. 5C). The distance

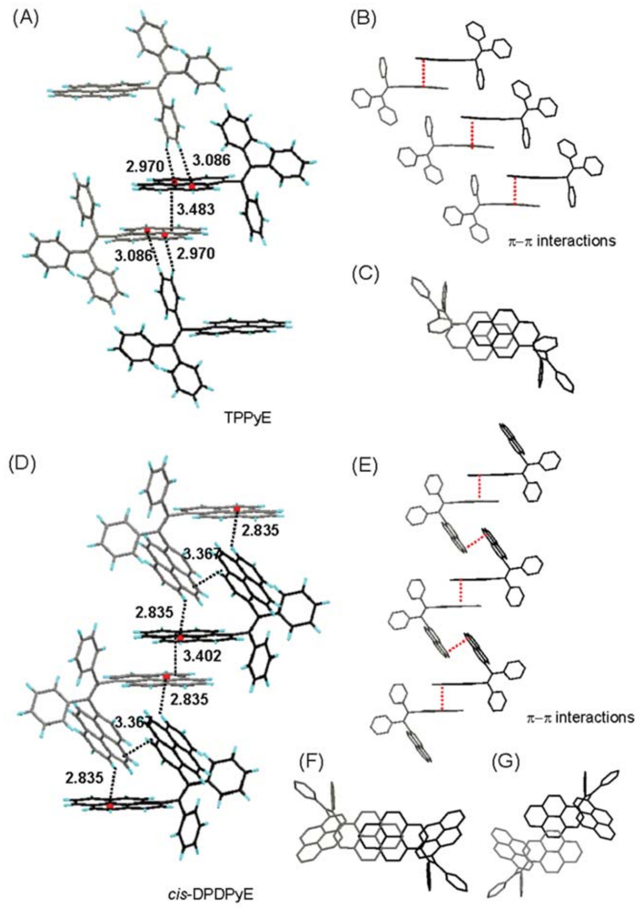

Fig. 5 (A) and (D) C–H$\cdots\pi$ hydrogen bonds and π–π interactions with indicated distances (Å) between the adjacent molecules of TPPyE and *cis*-DPDPyE in the crystal state. (B) and (E) Side and (C), (F) and (G) top views of adjacent molecules of TPPyE and *cis*-DPDPyE along the plane of pyrene stacking.

between two pyrene planes is 3.483 Å, which is shorter than the typical distance for π–π interaction (3.5 Å). Similar packing with a interplanar distance of 3.402 Å is also observed in the crystals of *cis*-DPDPyE. This provides evidence that the PL of TPPyE and *cis*-DPDPyE in the crystal state arises from the pyrene excimers (Fig. 5F). The second pyrene ring of *cis*-DPDPyE is also located parallel to the pyrene blade of its neighboring molecule with a spacing of 3.367 Å (Fig. 5D). Although the extent of overlapping is not so large, it helps to hinder the free rotation of the aromatic rings (Fig. 5G). Moreover, since both pyrene rings in one *cis*-DPDPyE molecule can form π–π stacking, the luminogen can self-assemble into a supermolecular structure (Fig. 5E) resembling that of a J-aggregate.[4f,15] Such behavior is also possible in concentrated solution, and it may be even easier for the molecules to form short dimer or trimer chains in a similar stacking pattern *via* maximized π–π intermolecular interactions. This may account for the red-shifted emission of the dye molecule in the solution state. However, such head-to-tail packing is not observed in TPPyE because there is only one pyrene ring in the molecule (Fig. 5B). The absence of such a linkage may lead to similar emission behaviors in the solution, amorphous and crystal states. Nevertheless, the crystal structure analysis has excluded the possibility of H-aggregate formation that leads to emission quenching of the luminogens.[4f,15] In addition to π–π stacking, multiple C–H$\cdots\pi$ hydrogen bonds with distances of 2.970 and 3.086 Å are formed between the hydrogen atoms of the phenyl rings in one TPPyE molecule and the π cloud of the pyrene ring in another molecule. C–H$\cdots\pi$ hydrogen bonds with a distance of 2.835 Å are also observed between the hydrogen atoms of the pyrene ring in one *cis*-DPDPyE molecule and the π cloud of the pyrene ring in another molecule. These weak but attractive forces of multiple C–H$\cdots\pi$ hydrogen bonds plus π–π interactions help rigidify the molecular conformation and lock the molecular rotations.[2,6] As a result, the excited energy consumed by the IMR process is greatly reduced, enabling TPPyE and DPDPyE to emit efficiently in the solid state.

The efficient PL of TPPyE and DPDPyE in the aggregate state prompted us to investigate their electroluminescence (EL). Multilayer non-doped organic light-emitting diodes (OLEDs) with configurations of ITO|NPB (60 nm)|TPPyE or DPDPyE (20 nm)|TPBi (30 nm)|LiF (1 nm)|Al (100 nm) (device I) and ITO|NPB (60 nm)|TPPyE or DPDPyE (20 nm)|TPBi (10 nm)|Alq$_3$ (30 nm)|LiF (1 nm)|Al (100 nm) (device II) were fabricated. In these EL devices, TPPyE and DPDPyE act as light emitters, *N*,*N*-bis(1-naphthyl)-*N*,*N*-diphenylbenzidine (NPB) functions as a hole-transport material and 2,2′,2″-(1,3,5-benzinetriyl)tris(1-phenyl-1-*H*-benzimidazole) (TPBi) and/or tris(8-hydroxyquinolinolato) aluminium (Alq$_3$) serve as hole-block and/or electron-transport materials, respectively. The device performances are summarized in Table 2. The EL spectra of TPPyE and DPDPyE show peaks at 504–520 nm, which are slightly red-shifted from the PL of their amorphous films due to the microcavity effect (Fig. 4B). In device I, TPPyE and DPDPyE turn-on at 4.6 and 5.3 V, exhibiting maximum luminance of 15450 and 45550 cd m^{-2} and current efficiency of 3.7 and 9.1 cd A^{-1}, respectively (Fig. 6A and 6B). The maximum external quantum efficiency (2.9%) attained by the device of DPDPyE is more than two times higher than the value achieved in TPPyE, presumably due to its higher solid-state Φ_F value and enhanced carrier mobility arising from the π–π stacking interactions between the pyrene rings. Even better EL performances are observed in device II. The DPDPyE device starts to emit at a low voltage of 3.2 V and radiates brilliantly with maximum luminance of 49830 cd cm^{-2} (Fig. 6C) and power, current and external quantum efficiencies of 9.2 lm W^{-1}, 10.2 cd A^{-1} and 3.3%, respectively (Fig. 6D). Similar large enhancement in the device performance is also observed in TPPyE, thanks to the additional Alq$_3$ layer, which improves the electron transportation in the EL device.

So far, there are several reports on high-efficiency green OLEDs fabricated using a doping method. For example, phosphorescent green OLEDs with a standard bottom-emitting structure can attain current efficiency over 60 cd A^{-1}. For those with advanced structures utilizing a host-dopant emitting layer such as CBP : Ir(ppy)$_3$, the power, current and external quantum efficiencies can reach 194 cd A^{-1}, 210 lm W^{-1} and 56.9%, respectively.[16] For fluorescent green OLEDs based on Alq$_3$: C545T, a high current efficiency of 24 cd A^{-1} can be achieved due to triplet–triplet annihilation.[17] However, the fabrication of these devices requires a strict control on the dopant concentration. If the concentration is too high, the energy transfer efficiency will be limited by concentration quenching and phase separation. The complicated fabrication process of the

Table 2 EL performances of TPPyE and DPDPyE.[a]

	Device	λ_{EL}/nm	V_{on}/V	L_{max}/cd m^{-2}	$\eta_{P,max}$/lm W^{-1}	$\eta_{C,max}$/cd A^{-1}	$\eta_{ext,max}$ (%)
TPPyE	I	508	4.6	15450	2.1	3.7	1.4
DPDPyE	I	520	5.3	45550	4.1	9.1	2.9
TPPyE	II	504	4.6	25470	2.7	4.0	2.0
DPDPyE	II	516	3.2	49830	9.2	10.2	3.3

[a] Abbreviations: V_{on} = turn-on voltage at 1 cd m^{-2}, L_{max} = maximum luminance, $\eta_{P,max}$, $\eta_{C,max}$ and $\eta_{ext,max}$ = maximum power, current and external quantum efficiencies, respectively.

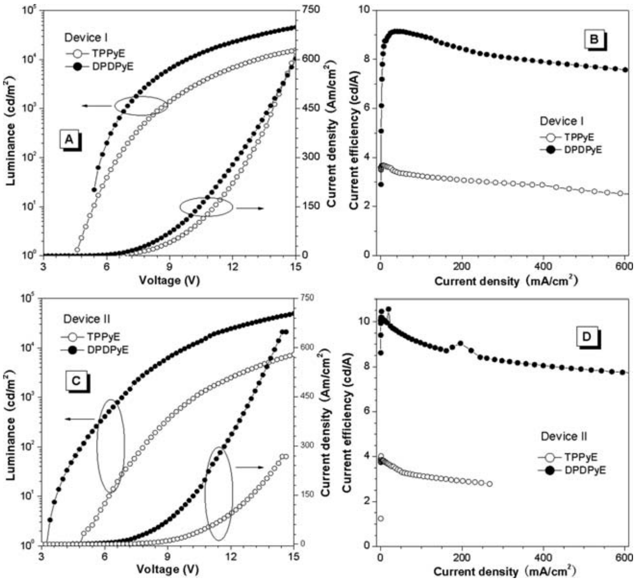

Fig. 6 Change in luminance (A) and current density (C) with the applied voltage and current efficiency *vs.* current density curves in devices I (B) and II (D).

doped OLEDs makes them unsuitable for rapid and mass production. Highly efficient green fluorescent emitters for non-doped OLEDs are in great demand for commercialization but unfortunately there are only few routes available in the literature that present the fabrication of efficient non-doped green OLEDs. Recently, Lee and co-workers[18] demonstrated a non-doped green OLED constructed from a dually functional material, phenyl-9-[8-(7,10-diphenylfluoranthenyl)]phenylcarbazole, that displays impressive high current efficiency of 10.1 cd A^{-1} and power efficiency of 12.1 lm W^{-1}. Wong and co-workers[19] reported an optimal device fabricated using 9,9-diarylfluorene-terminated 2,1,3-benzothiadiazole as green emitter and two triaryldiamines as hole transporters, which exhibits a maximum current efficiency of 12.9 cd A^{-1} and power efficiency of 11 lm W^{-1}. Although the device configuration is yet to be optimized, the performances of the devices based on our new molecules are outstanding compared with those of current non-doped green OLEDs. The EL efficiencies of DPDPyE (10.2 cd A^{-1} and 9.2 lm W^{-1}) are much better than those of Alq$_3$,[12c,20] a widely investigated green emitter. The values are also superior to those of commercial pyrene-based light-emitting materials,[11a,b] clearly demonstrating the high potential of the present molecules as solid emitters for the construction of efficient EL devices. An additional merit of our luminophors is that they can be readily synthesized by simple synthetic procedures, enabling them to find practical applications in electronics.

Conclusions

In summary, two pyrene-substituted ethenes are synthesized and their photophysical properties in solution and aggregate states are investigated. Both luminogens are weakly emissive in the solutions but become strong emitters when aggregated in the condensed phase. In contrast to the general observation that excimer formation quenches the light emissions of luminophors, both TPPyE and DPDPyE exhibit efficient excimer emissions in the solid state with high Φ_F values up to 100%. The π–π intermolecular interactions between the pyrene rings and the multiple C–H···π hydrogen bonds have efficiently restricted the IMR process of the molecules, which block the nonradiative energy decay channels, and thus enable them to emit intensely in the solid state. Multilayer devices using TPPyE and DPDPyE as host emitters are fabricated, which exhibit outstanding performances. The DPDPyE-based devices show low turn-on voltage (down to 3.2 V) with high luminance (up to 49830 cd m^{-2}) and power, current and external quantum efficiencies (up to 9.2 lm W^{-1}, 10.2 cd A^{-1} and 3.3%, respectively), making the present luminogens promising materials for the construction of efficient non-doped green OLEDs.

Experimental

Materials and instrumentation

THF was distilled from sodium benzophenone ketyl under dry nitrogen immediately prior to use. All other chemicals and reagents were purchased from Aldrich and used as received without further purification. ^{1}H and ^{13}C NMR spectra were measured on a Bruker AV 300 spectrometer in deuterated chloroform using tetramethylsilane (TMS; δ = 0) as internal reference. UV spectra were measured on a Milton Roy Spectronic 3000 Array spectrophotometer. PL spectra were recorded on a Perkin-Elmer LS 55 spectrofluorometer. High-resolution mass spectra (HRMS) were recorded on a GCT premier CAB048 mass spectrometer operating in MALDI-TOF mode. Elemental analysis was performed on an Elementary Vario EL analyzer. Single-crystal X-ray diffraction intensity data were collected on a Bruker–Nonices Smart Apex CCD diffractometer with graphite-monochromated Mo-Kα radiation. Processing of the intensity data was carried out using the SAINT and SADABS routines, and the structure and refinement were conducted using the SHELTL suite of X-ray programs (version 6.10). TGA analysis was carried on a TA TGA Q5000 under dry nitrogen at a heating rate of 10 °C min^{-1}. Thermal transitions were investigated by a TA DSC Q1000 under dry nitrogen at a heating rate of 10 °C min^{-1}. The ground-state geometries were optimized using the density functional with B3LYP hybrid functional at the basis set level of 6-31G*. All the calculations were performed using the Gaussian 03 package. ED patterns were obtained using a JOEL 2010 transmission electron microscope at an accelerating voltage of 200 kV. Samples were prepared by drop-casting dilute suspensions onto a copper 400-mesh carrier grid covered with carbon-coated formvar film and dried in open air at room temperature.

Device fabrication

The devices were fabricated on 80 nm-ITO coated glass with a sheet resistance of 25 $\Omega\ \square^{-1}$. Prior to loading into the pretreatment chamber, the ITO-coated glass was soaked in ultrasonic detergent for 30 min, followed by spraying with de-ionized water for 10 min, soaking in ultrasonic de-ionized water for 30 min, and oven-baking for 1 h. The cleaned samples were treated by perfluoromethane plasma with a power of 100 W, gas flow of 50 sccm, and pressure of 0.2 Torr for 10 s in the pretreatment chamber. The samples were transferred to the organic chamber with a base pressure of 7×10^{-7} Torr for the deposition of NPB, emitter, TPBi, and/or Alq$_3$, which served as hole-transport, light-emitting, hole-block, and/or electron-transport layers, respectively. The samples were then transferred to the metal chamber for cathode deposition to lithium fluoride (LiF) capped with aluminium (Al). The light-emitting area was 4 mm^2. The current density–voltage characteristics of the devices were measured by a HP4145B semiconductor parameter analyzer. The forward direction photons emitted from the devices were detected by a calibrated UDT PIN-25D silicon photodiode. The luminance and external quantum efficiencies of the devices were inferred from the photocurrent of the photodiode. The electroluminescence spectra were obtained by a PR650 spectrophotometer. All measurements were carried out under air at room temperature without device encapsulation.

Preparation of nanoaggregates

Stock THF solutions of TPPyE and DPDPyE with a concentration of 10^{-5} M were prepared. Aliquots of the stock solution were transferred to 10 mL volumetric flasks. After appropriate amounts of THF were added, water was added dropwise under vigorous stirring to furnish 10^{-6} M solutions with different water contents (0–99.5 vol%). The PL measurements of the resultant solutions were then performed immediately.

X-Ray crystallography

Crystal data for TPPyE. $C_{36}H_{24}$, $M_r = 456.55$, triclinic, $P\bar{1}$, $a = 9.5346(6)$, $b = 9.5932(6)$, $c = 13.9476(9)$ Å, $\alpha = 96.674(5)$, $\beta = 105.479(6)$, $\gamma = 94.841(5)°$, $V = 1212.24(13)$ Å^3, $Z = 2$, $D_c = 1.251$ g cm^{-3}, $\mu = 0.537$ mm^{-1} (Mo-Kα, $\lambda = 1.54178$), $F(000) = 480$, $T = 173(2)$ K, $2\theta_{max} = 66.5°$ (95.1%), 6354 measured reflections, 4112 independent reflections ($R_{int} = 0.0277$), GOF on $F^2 = 1.012$, $R_1 = 0.0476$, w$R_2 = 0.0994$ (all data), $\Delta\rho_{max,min} =$ 0.148 and −0.183 e Å^{-3}.

Crystal data for *cis*-DPDPyE. $C_{46}H_{28}\cdot CHCl_3$, $M_r = 700.05$, triclinic, $P\bar{1}$, $a = 8.7695(6)$, $b = 13.3414(11)$, $c = 15.9829(11)$ Å, $\alpha = 77.119(8)$, $\beta = 89.166(6)$, $\gamma = 71.187(6)°$, $V = 1722.2(2)$ Å^3, $Z = 2$, $D_c = 1.350$ g cm^{-3}, $\mu = 2.667$ mm^{-1} (Mo-Kα, $\lambda = 1.54178$), $F(000) = 724$, $T = 173(2)$ K, $2\theta_{max} = 66.5°$ (95.1%), 8722 measured reflections, 5520 independent reflections ($R_{int} = 0.0649$), GOF on $F^2 = 1.076$, $R_1 = 0.0875$, w$R_2 = 0.2066$ (all data), $\Delta\rho_{max,min} =$ 0.515 and −0.356 e Å^{-3}.

Synthesis

Pyrenophenone (2). To a solution of pyrene (2 g, 10 mmol) and aluminium(III) chloride (1.6 g, 12 mmol) in dry dichloromethane (100 mL) was added dropwise benzoyl chloride (1.4 g, 10 mmol) at 0 °C. The resultant black solution was stirred overnight at room temperature. The solution was poured into water and extracted with dichloromethane. The organic layer was washed with saturated brine solution and dried over anhydrous magnesium sulfate. After filtration and solvent evaporation, the residue was purified by silica-gel column chromatography using *n*-hexane–dichloromethane as eluent. Orange solid **2** was obtained in 80% yield (2.4 g). ^{1}H NMR (300 MHz, CDCl$_3$), δ (TMS, ppm): 8.36 (d, 1H, J = 9.27 Hz), 8.27–8.17 (m, 4H), 8.13–8.03 (m, 4H), 7.92–7.89 (m, 2H), 7.65–7.60 (m, 1H), 7.51–7.46 (m, 2H). ^{13}C NMR (75 MHz, CDCl$_3$), δ (TMS, ppm): 199.1, 139.4, 133.8, 133.77, 133.74, 131.8, 131.33, 131.28, 130.4, 129.8, 129.6, 129.1, 127.9, 127.6, 127.1, 126.7, 126.6, 125.5, 125.4, 124.4. HRMS (MALDI-TOF): *m*/*z* 306.2141 (M$^+$, calc. 306.1045). Anal. Calc, for $C_{23}H_{14}O$: C, 90.17; H, 4.61; O, 5.22. Found: C, 90.12; H, 4.48; O, 5.52%; mp 118 °C.

1,2,2-Triphenyl-1-pyrenylethene (TPPyE). To a solution of diphenylmethane (1 g, 6 mmol) in dry THF (30 mL) was added dropwise a 1.6 M solution of *n*-butyllithium in hexane (3.7 mL, 6 mmol) at 0 °C under nitrogen. After stirring for 1 h at 0 °C, the resultant orange–red solution was transferred slowly to a solution of **2** (1.5 g, 5 mmol) in THF (20 mL) at 0 °C. The reaction mixture was allowed to warm to room temperature and stirred for 6 h. The reaction was quenched with aqueous ammonium chloride solution. The organic layer was extracted with dichloromethane and the combined organic layers were washed with saturated brine solution and dried over anhydrous magnesium sulfate. After filtration and solvent evaporation, the resultant crude alcohol with excess diphenylmethane was dissolved in about 50 mL of toluene. A catalytic amount of *p*-toluenesulfonic acid (0.25 g, 1.3 mmol) was then added. After heating under reflux for 6 h, the mixture was cooled to room temperature, washed with saturated brine solution and water, and dried over anhydrous magnesium sulfate. After filtration and solvent evaporation, the residue was purified by silica-gel column chromatography using *n*-hexane–dichloromethane as eluent. Pale yellow solid of TPPyE was obtained in 72% yield (1.6 g). ^{1}H NMR (300 MHz, CDCl$_3$), δ (TMS, ppm): 8.29 (d, 1H, J = 9.3 Hz), 8.15–8.08 (m, 2H), 8.03–7.91 (m, 5H), 7.82 (d, 1H, J = 7.8 Hz), 7.24–7.20 (m, 5H), 7.06–9.67 (m, 7H), 6.83–6.80 (m, 3H). ^{13}C NMR (75 MHz, CDCl$_3$), δ (TMS, ppm): 144.3, 144.23, 144.19, 144.0, 140.1, 139.7, 139.3, 132.2, 131.9, 131.6, 131.4, 131.1, 130.5, 130.9, 128.6, 128.4, 128.1, 128.0, 127.7, 127.5, 127.1, 126.5, 126.2, 125.6, 125.5, 125.2. HRMS (MALDI-TOF): *m*/*z*

456.2043 (M$^+$, calc. 456.1878). Anal. Calc. for $C_{36}H_{24}$: C, 94.70; H, 5.30. Found: C, 94.58; H, 5.51%; mp 203 °C.

1,2-Diphenyl-1,2-dipyrenylethene (DPDPyE). To a solution of **2** (1.5 g, 5 mmol) and zinc dust (0.65 g, 10 mmol) in 50 mL dry THF was added dropwise titanium(IV) chloride (0.95 g, 5 mmol) under nitrogen at -78 °C. After stirring for 20 min, the reaction mixture was warmed to room temperature and then heated to reflux for 12 h. The reaction mixture was then cooled to room temperature and poured into water. The organic layer was extracted with dichloromethane and the combined organic layers were washed with saturated brine solution and water and dried over anhydrous magnesium sulfate. After filtration and solvent evaporation, the residue was purified by silica-gel column chromatography using *n*-hexane–dichloromethane as eluent. Pale yellow solid of DPDPyE was obtained in 56% yield (0.81 g). ^{1}H NMR (300 MHz, $CDCl_3$), δ (TMS, ppm): 8.48–8.40 (m, 2H), 8.20–7.95 (m, 16H), 7.01–6.96 (m, 4H), 6.83–6.74 (m, 6H). HRMS (MALDI-TOF): *m*/*z* 580.4069 (M$^+$, calc. 580.2129). Anal. Calc. for $C_{46}H_{28}$: C, 95.14; H, 4.86. Found: C, 94.87; H, 4.96%; mp 279 °C.

Acknowledgements

This project was partially supported by grants from the Research Grants Council of Hong Kong (603509, 601608, CUHK2/CRF/08, and HKUST2/CRF/10), the Innovation and Technology Commission (ITP/008/09NP and ITS/168/09), the University Grants Committee of Hong Kong (AoE/P-03/08), and the National Science Foundation of China (20974028). B. Z. T. acknowledges support from the Cao Gaungbiao Foundation of Zhejiang University. Z. J. Z. acknowledges financial support from the Initial Funding of Hangzhou Normal University (HSQK0085).

References

1 (*a*) M. D. Watson, F. Jäckel, N. Severin, J. P. Rabe and K. Müllen, *J. Am. Chem. Soc.*, 2004, **126**, 1402; (*b*) H. Zhang, Y. Wang, K. Shao, Y. Lin, S. Chen, W. Qiu, X. Sun, T. Qi, Y. Ma, G. Yu, Z. Su and D. Zhu, *Chem. Commun.*, 2006, 755; (*c*) W.-L. Jia, T. McCormick, Q.-D. Lin, H. Fukutani, M. Motala, R.-Y. Wang, Y. Tao and S. Wang, *J. Mater. Chem.*, 2004, **14**, 3344; (*d*) J. E. Anthony, *Chem. Rev.*, 2006, **106**, 5028.

2 (*a*) R. Nandy, M. Subramoni, B. Varghese and S. Sankararaman, *J. Org. Chem.*, 2007, **72**, 938; (*b*) S. Sankararaman, G. Venkataramana and B. Varghese, *J. Org. Chem.*, 2008, **73**, 2404.

3 (*a*) A. C. Grimsdale, K. L. Chan, R. E. Martin, P. G. Jokisz and A. B. Holmes, *Chem. Rev.*, 2009, **109**, 897; (*b*) J. Liu, J. W. Y. Lam and B. Z. Tang, *Chem. Rev.*, 2009, **109**, 5799.

4 (*a*) J. Luo, Z. Xie, J. W. Y. Lam, L. Cheng, H. Chen, C. Qiu, H. S. Kwok, X. Zhan, Y. Liu, D. Zhu and B. Z. Tang, *Chem. Commun.*, 2001, 1740; (*b*) M. Shimizu, H. Tatsumi, K. Mochida, K. Shimono and T. Hiyama, *Chem.–Asian J.*, 2009, **4**, 1289; (*c*) A. Iida and S. Yamaguchi, *Chem. Commun.*, 2009, 3002; (*d*) M. Shimizu, Y. Takeda, M. Higashi and T. Hiyama, *Angew. Chem., Int. Ed.*, 2009, **48**, 3653; (*e*) M. Levitus, K. Schmieder, H. Ricks, K. D. Shimizu, U. H. F. Bunz and M. A. Garcia-Garibay, *J. Am. Chem. Soc.*, 2001, **123**, 4259; (*f*) B.-K. An, S.-K. Kwon, S.-D. Jung and S. Y. Park, *J. Am. Chem. Soc.*, 2002, **124**, 14410; (*g*) C. Belton, D. F. O'Brien, W. J. Blau, A. J. Cadby, P. A. Lane, D. D. C. Bradley, H. J. Byrne, R. Stockmann and H.-H. Hörhold, *Appl. Phys. Lett.*, 2001, **78**, 1059; (*h*) L. Antolini, E. Tedesco, G. Barbarella, L. Favaretto, G. Sotgiu, M. Zambianchi, D. Casarini, G. Gigli and R. Cingolani, *J. Am. Chem. Soc.*, 2000, **122**, 9006; (*i*) R. Deans, J. Kim, M. R. Machacek and T. M. Swager, *J. Am. Chem. Soc.*, 2000, **122**, 8565; (*j*) T. P. I. Saragi, T. Spehr, A. Siebert, T. Fuhrmann-Lieker and J. Salbeck, *Chem. Rev.*, 2007, **107**, 1011.

5 (*a*) Z. Li, Y. Dong, B. Mi, Y. Tang, M. Häussler, H. Tong, P. Dong, J. W. Y. Lam, Y. Ren, H. H. Y. Sun, K. Wong, P. Gao, I. D. Williams, H. S. Kwok and B. Z. Tang, *J. Phys. Chem. B*, 2005, **109**, 10061; (*b*) G. Yu, S. Yin, Y. Liu, J. Chen, X. Xu, X. Sun, D. Ma, X. Zhan, Q. Peng, Z. Shuai, B. Z. Tang, D. Zhu, W. Fang and Y. Luo, *J. Am. Chem. Soc.*, 2005, **127**, 6335; (*c*) Z. Zhao, S. Chen, J. W. Y. Lam, C. K. W. Jim, C. Y. K. Chan, Z. Wang, P. Lu, H. S. Kwok, Y. Ma and B. Z. Tang, *J. Phys. Chem. C*, 2010, **114**, 7963.

6 (*a*) Z. Zhao, Z. Wang, P. Lu, C. Y. K. Chan, D. Liu, J. W. Y. Lam, H. H. Y. Sung, I. D. Williams, Y. Ma and B. Z. Tang, *Angew. Chem., Int. Ed.*, 2009, **48**, 7608; (*b*) H. Tong, Y. Dong, Y. Hong, M. Haeussler, J. W. Y. Lam, H. H. Y. Sung, X. Yu, J. Sun, I. D. Williams, H. S. Kwok and B. Z. Tang, *J. Phys. Chem. C*, 2007, **111**, 2287; (*c*) Z. Zhao, P. Lu, J. W. Y. Lam, Z. Wang, C. Y. K. Chan, H. H. Y. Sung, I. D. Williams, Y. Ma and B. Z. Tang, *Chem. Sci.*, 2011, **2**, 672.

7 (*a*) F. M. Winnik, *Chem. Rev.*, 1993, **93**, 587; (*b*) J. B. Birks, *Photophysics of Aromatic Molecules*, Wiley-Interscience, London, 1970; (*c*) J. R. Lakowicz, *Principles of Fluorescence Spectroscopy*, Plenum Press, New York, 1999.

8 (*a*) S. H. Lee, S. H. Kim, S. K. Kim, J. H. Jung and J. S. Kim, *J. Org. Chem.*, 2005, **70**, 9288; (*b*) S. Nishizawa, Y. Kato and N. Teramae, *J. Am. Chem. Soc.*, 1999, **121**, 9463; (*c*) T.-C. Chou, C.-L. Hwa, J.-J. Lin, K.-C. Liao and J.-C. Tseng, *J. Org. Chem.*, 2005, **70**, 9717; (*d*) I. Suzuki, M. Ui and A. Yamauchi, *J. Am. Chem. Soc.*, 2006, **128**, 4498.

9 I. B. Berlman, *Handbook of Fluorescence Spectra of Aromatic Molecules*, Academic Press, New York and London, 1971.

10 J. A. Mikroyannidis, L. Fenenko and C. Adachi, *J. Phys. Chem. B*, 2006, **110**, 20317.

11 (*a*) K.-C. Wu, P.-J. Ku, C.-S. Lin, H.-T. Shih, F.-I. Wu, M.-J. Huang, J.-J. Lin, I.-C. Chen and C.-H. Cheng, *Adv. Funct. Mater.*, 2008, **18**, 67; (*b*) S. T. Tao, Z. K. Peng, X. H. Zhang, P. F. Wang, C.-S. Lee and S.-T. Lee, *Adv. Funct. Mater.*, 2005, **15**, 1716; (*c*) C. Tang, F. Liu, Y.-J. Xia, L.-H. Xie, A. Wei, S.-B. Li, Q.-L. Fan and W. Huang, *J. Mater. Chem.*, 2006, **16**, 4074; (*d*) M. Y. Lo, C. Zhen, M. Lauters, G. E. Jabbour and A. Sellinger, *J. Am. Chem. Soc.*, 2007, **129**, 5808; (*e*) Z. Zhao, J.-H. Li, P. Lu and Y. Yang, *Adv. Funct. Mater.*, 2007, **17**, 2203.

12 (*a*) Y. Dong, J. W. Y. Lam, A. Qin, J. Liu, Z. Li, B. Z. Tang, J. Sun and H. S. Kwok, *Appl. Phys. Lett.*, 2007, **91**, 011111; (*b*) Z. Zhao, S. Chen, X. Shen, F. Mahtab, Y. Yu, P. Lu, J. W. Y. Lam, H. S. Kwok and B. Z. Tang, *Chem. Commun.*, 2010, **46**, 686; (*c*) Z. Zhao, S. Chen, J. W. Y. Lam, P. Lu, Y. Zhong, K. S. Wong, H. S. Kwok and B. Z. Tang, *Chem. Commun.*, 2010, **46**, 2221; (*d*) W. Yuan, P. Lu, S. Chen, J. W. Y. Lam, Z. Wang, Y. Liu, H. S. Kwok, Y. Ma and B. Z. Tang, *Adv. Mater.*, 2010, **22**, 2159; (*e*) Z. Zhao, J. W. Y. Lam and B. Z. Tang, *Curr. Org. Chem.*, 2010, **14**, 2109.

13 M. Knaapila, R. C. Evans, V. M. Garamus, L. Almásy, N. K. Székely, A. Gutacker, U. Scherf and H. D. Burrows, *Langmuir*, 2010, **26**, 15634.

14 (*a*) J. B. Birks, A. A. Kazzaz and T. A. King, *Proc. R. Soc. London, Ser. A*, 1966, **291**, 556; (*b*) T. Seko, K. Ogura, Y. Kawakami, H. Sugino, H. Toyotama and J. Tanaka, *Chem. Phys. Lett.*, 1998, **291**, 438; (*c*) R. Katoh, K. Suzuki, A. Furube, M. Kotani and K. Tokumaru, *J. Phys. Chem. C*, 2009, **113**, 2961.

15 (*a*) S. Zhang, Y. Guo, L. Wang, Q. Li, K. Zheng, X. Zhan, Y. Liu, R. Liu and L.-J. Wan, *J. Phys. Chem. C*, 2009, **113**, 16232; (*b*) S. Ghosh, X.-Q. Li, V. Stepanenko and F. Würthner, *Chem.–Eur. J.*, 2008, **14**, 11343.

16 A. Mikami and T. Koyanagi, *Dig. Tech. Pap. - Soc. Inf. Disp. Int. Symp.*, 2009, **40**(1), 907.

17 J. Kidoa and Y. Iizumi, *Appl. Phys. Lett.*, 1998, **73**, 2721.

18 (*a*) Q.-X. Tong, S.-L. Lai, M.-Y. Chan, Y.-C. Zhou, H.-L. Kwong, C.-S. Lee and S.-T. Lee, *Chem. Phys. Lett.*, 2008, **455**, 79; (*b*) Q.-X. Tong, S.-L. Lai, M.-Y. Chan, K.-H. Lai, J.-X. Tang, H.-L. Kwong, C.-S. Lee and S.-T. Lee, *Appl. Phys. Lett.*, 2007, **91**, 153504.

19 S.-Y. Ku, L.-C. Chi, W.-Y. Hung, S.-W. Yang, T.-C. Tsai, K.-T. Wong, Y.-H. Chen and C.-I. Wu, *J. Mater. Chem.*, 2009, **19**, 773.

20 C. W. Tang and S. A. VanSlyke, *Appl. Phys. Lett.*, 1987, **51**, 913.